Adsorption of HF on gibbsite calcined at various temperatures. A solid-state NMR study of low-level fluorinated systems.

Gordon Agbenyegah[1, 2], Joshua P. Clark[3], John V. Hanna[3], Margaret Hyland[1, 2], James B. Metson[1,4], Grant McIntosh[1,4], Ronny Etzion[1], Graham A. Bowmaker[4] and Zoran Zujovic[*4,5]

[1]*Light Metals Research Centre, University of Auckland, Private Bag 92019, Auckland, New Zealand*

[2]*Department of Chemical and Materials Engineering, University of Auckland, Private Bag 92019, Auckland, New Zealand*

[3]*Department of Physics, University of Warwick, Coventry CV4 7AL, United Kingdom*

[4]*School of Chemical Sciences, University of Auckland, Private Bag 92019, Auckland, New Zealand*

[5]*NMR Centre, School of Chemical Sciences, the University of Auckland, Private Bag 92019, Auckland, New Zealand*

[*]Author to whom correspondence should be addressed. E-mail: z.zujovic@auckland.ac.nz; Tel.: +64-(0)9-923-8336

Abstract

The fluorination mechanism of low-level fluorinated materials obtained by calcination of Bayer gibbsite at different temperatures was studied using ^{27}Al and ^{19}F solid-state NMR (SSNMR) spectroscopy and X-Ray Diffraction (XRD). Gibbsite was calcined at 400, 600, 800 and 1000 ºC followed by treatment with anhydrous HF/N$_2$ gas at 100 °C. Three types of Al-F species on the surface of fluorinated gibbsite calcined at 400, 600, 800 ºC are proposed based on the ^{19}F MAS NMR spectra which show peaks at ca. −132, −137 and −163 ppm while the spectrum of the fluorinated gibbsite calcined at 1000 ºC showed five additional peaks at ca. −139, −164, −176, −183 and −191 ppm. The fluorination process in aluminas

is founded on elementary exchange reactions in which F[-] replaces surface -OH groups based on their basicity. The ^{27}Al magic angle spinning (MAS) NMR and ^{19}F-^{27}Al cross-polarization CP-MAS experiments confirmed the presence of octahedral Al species.

Introduction

Aluminum oxide (Al$_2$O$_3$, alumina) is a white powder produced by the refining of bauxite ore, which is found in large quantities in the earth's crust.[1] Because of its chemical and thermal stability and the opportunities to finely tune its physicochemical and textural properties (surface area, pore-volume, and pore size distribution), alumina has been extensively used as catalyst support.[2] Also, with surface modification, it can act as a useful catalyst in its own right.[3] Most notably, alumina is capable of providing acidic surface groups, which catalyze a broad range of chemical reactions.[2] Although still debated,[4] it is generally accepted that the alumina surface is widely hydroxylic in nature with about 20 OH groups per nm^2. The major industrial procedure for aluminum production is the electrolytic Hall-Heroult process. This process results in the emission of gaseous and particulate fluorides, which are captured by virgin or primary smelter-grade alumina (SGA) in a gas treatment centre (GTC) to safeguard humans and the environment.[5] Optimum fluoride content is also necessary to maintain the electrolyte chemistry as this affects the liquidus point of the electrolyte and the effective dissolution of alumina.

The structure of SGA at the micro-level is important for smelter operation in various key areas. One of these is the connection between the degree of calcination and the SGA microstructure (the thermal evolution of transitional alumina phases) in relation to dry-scrubber performance. The relationship between surface area and microstructure in the calcination of Bayer gibbsite has been reported.[6] To understand the balance between the HF production at the cell and the HF absorption in the scrubber, the relative rates of hydroxyl group loss versus a loss of surface area should be analyzed. This is important because the alumina demand of the dry-scrubbers typically exceeds that for reduction cell feeding, necessitating recycling of alumina in the scrubber. Therefore, a detailed understanding of

how fluoride adsorbs onto alumina surfaces, produced from gibbsite specimens calcined at various temperatures, is essential for smelters both regarding environmental footprint and production efficiency.

Solid-state MAS NMR of Fluoraluminate Materials

Fluorine (^{19}F) and aluminum (^{27}Al) solid-state NMR spectroscopy have been widely and successfully applied in the investigations of aluminas and various fluorinated aluminum-based materials.[7] ^{19}F NMR has been used to confirm the formation of AlF_3 in fluorinated γ-Al_2O_3 after high fluorine loading by NH_4HF_2 aqueous solutions.[8] _ENREF_2 The authors of this work were able to reveal three different Al-F species on the surface of γ-Al_2O_3. To support the spectral assignment of the ^{27}Al MAS NMR spectrum, Fischer *et al*. analyzed the AlF_3 reference sample using a 3QMAS (triple-quantum magic angle spinning) experiment.[8] König *et al*. used NMR measurements of the well-defined hydrated crystalline and amorphous aluminum hydroxy fluorides $AlF_x(OH)_{3-x} \cdot H_2O$ to correlate ^{19}F chemical shifts with the average chemical compositions of the AlF_xO_{6-x} species obtained by elemental analysis[9]. Well-defined crystalline aluminum hydroxy fluorides in the cubic pyrochlore structure $AlF_x(OH)_{3-x} \cdot H_2O$ with different fluorine contents are studied by using NMR spectroscopy at different magnetic field strengths.[10] Zhang *et al*. studied the fluorine species on the surface of fluorinated alumina obtained by impregnation of γ-Al_2O_3 with an aqueous solution of NH_4F.[11] Three fluorine species (fluorine coordinated by one, S1, two, S2, and three S3, octahedral aluminum atoms) were proposed. These authors concluded that fluorination at low fluoride loadings favors the removal of one coordinated hydroxyl, which produces S1 species. Chupas and Grey studied surface changes obtained in the fluorination reaction of aluminas with $CHClF_2$ using ^{19}F-^{27}Al Cross Polarization (CP), Multi-Quantum Magic Angle Spinning (MQMAS), and 2D Heteronuclear Chemical-Shift Correlation (HETCOR) experiments.[12] This group proposed a mechanism where the fluorination at the initial stage yields terminal single-bonded Al-F groups. One of the processes during fluorination is the conversion of coordinatively unsaturated pentahedral and tetrahedral aluminum atoms located in the near surface region, which leads to the formation of octahedral aluminum oxy-fluoride species.[12] Scalise *et al*. used solid-state NMR to reveal adsorbed fluorine structural units at the surfaces of unmilled and milled γ-

Al$_2$O$_3$ treated with 0.1 N NaF.[13] König *et al*. used high field Magic Angle Spinning (MAS) NMR up to 21.1 T which allowed them to detect both tetrahedral AlF$_x$O$_{4-x}$ and pentahedral AlF$_x$O$_{5-x}$ species in strongly disordered aluminum isopropoxide fluorides. They found that the amount of octahedral aluminum species increases, while the amount of the tetrahedral and pentahedral aluminum decreases during the course of fluorination in disordered aluminum isopropoxide fluorides.[14] Ahrem *et al*. investigated the thermal evolution of tetrahedral and pentahedral aluminum atoms in amorphous aluminum hydroxide fluorides with low degrees of fluorination.[15] Chupas *et al*. studied the fluorination of γ-alumina (γ-Al$_2$O$_3$) with HCF$_2$Cl and the formation of catalysts at high temperatures of 300 or 400 °C.[16] The application of ^{19}F/^{27}Al CP-MAS NMR techniques demonstrated that changes due to low levels of fluorination on the surface of the alumina could be studied by this technique.[16] Dando used ^{19}F solid-state NMR to study the fluoride adsorption mechanism in smelting grade alumina (SGA). These authors suggested that at the beginning of the fluorination process surface hydroxyls were replaced by adsorbed fluoride which produced single bonded aluminum oxyfluorides. Further fluorination leads to the displacement of bridging hydroxyls, yielding eventually the AlF$_3$ structures.[17]

A study of HF adsorption in a fluidized bed reactor can yield invaluable kinetic and design data useful for the prediction of scrubbing efficiency and GTC performance. HF is a common flue gas component generated by the reaction of hydrogen (from adsorbed water on alumina feeds, humidity, or in the carbon anodes) with the fluoride electrolyte.[18] The coordinatively unsaturated aluminum defect sites on alumina surfaces[19], serve as possible adsorption sites for polar compounds such as water and HF. The surface defect domains in aluminas are argued to be the reaction sites where HF gas reacts to form aluminum hydroxyfluoride.[20] For GTC applications, aluminas with the large specific surface area (60 – 80m^2/g) are preferred.[21]

In general, the mechanism of fluorination of the surface of aluminas will depend on the surface structure and chemistry and the characteristics of fluorinating species produced in the process. The aim of this work was to synthesize a series of gibbsite specimens calcined at various temperatures and explore how the temperature affects the adsorption properties of corresponding aluminas and what impact the fluorination process has on local aluminum coordination. Therefore, XRD on the gibbsite

calcined at various temperatures and ^{27}Al MAS NMR, ^{19}F-^{27}Al CP-MAS and ^{19}F MAS NMR solid-state NMR measurements on these and related HF adsorption products were performed to analyze the process of low-level fluorination.

Experimental section

Aluminas were produced by calcination of Bayer gibbsite in a horizontal tube furnace in open crucibles in the air with hold times of 24 hr. All samples were placed into a furnace preheated to 400, 600, 800 and 1000 ºC and removed after the determined hold time to cool under ambient conditions without quenching. One gram of the variably calcined gibbsite specimens or smelter grade alumina was reacted with HF gas in a fluidized bed reactor. The reactor was a cylindrical stainless-steel column (16.5 cm long × 1.5 cm ID) lined with an HF-resistant fluoropolymer. Porous Teflon retaining frits were installed at the reactor inlet and outlet to prevent alumina entrainment in the gas stream. A mixture of 1400 ppm HF in nitrogen was diluted with preheated nitrogen gas in a mixing tee to attain 400 ppm of dry HF/N$_2$ via high precision mass flow controllers. A reaction temperature of 100 ºC was maintained by enclosing the reactor, tubes (copper and PTFE) and all fittings in an oven. The temperature was measured using an N-type thermocouple installed on the copper tubes and at the reactor outlet. The HF concentration was continuously measured in a Teflon gas cell (20 cm path length) with a Boreal Laser GasFinder™ 2.0 HF monitor, and the exiting gas continuously bubbled through a suspension of Ca(OH)$_2$ for disposal. Experiments were considered complete when the reactor exit HF concentration measured 10 ppm. This was referred to as the 'breakthrough point', at which point the HF capture efficiency is significantly lower than 100%.

XRD

X-ray powder diffraction (XRD) patterns were recorded on a Rigaku Miniflex II Desktop X-ray powder diffractometer using monochromated Cu Kα radiation (λ = 1.541 Å, 30 kV, 15 mA) over the 2θ range 10 – 80° at a step size of 0.2°.

Solid-state NMR Spectroscopy

The ^{19}F data were measured at 2.35 T using a Bruker HD-100 spectrometer (Larmor frequency $\nu_L(^{19}F)$ = 94.20 MHz) and a Bruker 1.3 mm HX MAS NMR probe, which enabled a MAS frequency of ν_{rot} = 60 kHz. A rotor-synchronized Hahn-Echo experiment was implemented with a $\pi/2$ and π pulses of 2.5 and 5.0 µs duration, respectively, a rotor-synchronized τ delay of 12.9 µs, and a recycle delay of 2 s. All ^{19}F chemical shifts are reported against the IUPAC $CFCl_3$ primary standard, and each spectrum was fitted using Origin Pro® 9 software. The corresponding ^{27}Al MAS NMR data were acquired at 9.4 T using a Bruker HD-400 spectrometer (Larmor frequency $\nu_L(^{27}Al)$ = 103.92 MHz) and a Bruker 3.2 mm HX MAS NMR probe which delivered a MAS frequency of 20 kHz. The recycle delay was 2 s and the number of transients was 14336

The ^{19}F-^{27}Al CPMAS and ^{27}Al MAS NMR spectra were measured at 11.7 T on a Bruker Avance III-500 spectrometer (Larmor frequencies $\nu_L(^{27}Al)$ = 130.34 MHz, $\nu_L(^{19}F)$ = 470.59 MHz), using a 4 mm Bruker HX MAS probe. The excitation pulse for ^{27}Al MAS NMR experiment was 0.7 µs ($\leq \pi/12$) with repetition times of 2 s. The number of transients was 256. The Hartmann–Hahn condition for the ^{19}F-^{27}Al CP MAS experiments was determined with $AlF_3 \cdot 3H_2O$ and adjusted for the fast-spinning regime,[22] using a radio frequency field strength for ^{27}Al of 15 kHz. ^{19}F-^{27}Al RAMP-CP (ramped amplitude cross-polarization) and ^{19}F SPINAL-64 decoupling scheme was applied. A rotor synchronized contact time of 133 µs was used for MAS frequencies of 15 kHz, with repetition times of 10 s. The number of transients was 32 The offset frequency of the ^{19}F radio-frequency field was varied to check for the ^{27}Al signals originating from tetrahedral fluorine structures. The number of transients was 5920. The ^{27}Al chemical shifts scale was referenced to $AlCl_3$ in aqueous solution (0 ppm).

Results and Discussion

XRD measurements

The XRD powder diffractograms of the gibbsite calcined at various temperatures are shown in Figure 1. The diffractogram of the sample calcined to 400 °C indicate the presence of both crystalline and amorphous phases. The sharp diffraction peaks from the phase with the long-range order can be attributed to the boehmite while the broad ones can be assigned to the presence of the disordered boehmite framework and the possible presence of γ-Al_2O_3. This disordered structure is formed during

the decomposition of gibbsite crystallites caused by the increase of pressure and rapid water expulsion.[23] At higher temperatures (600 and 800 °C), the diffractograms imply the presence of the γ-Al_2O_3 as a major component. The diffractogram of the sample calcined at 1000 °C reveals much higher crystallinity and is much more complex, revealing the presence of the α-Al_2O_3, θ-Al_2O_3 and δ-Al_2O_3.[23]
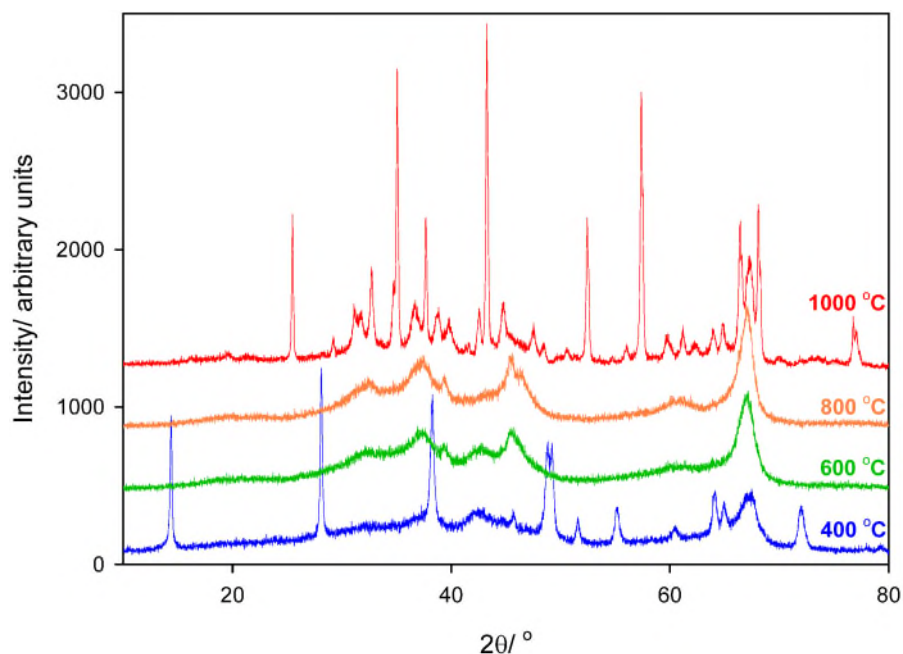
Figure 1. XRD powder diffractograms of the gibbsite precursors calcined at various temperatures.

^{27}Al MAS NMR and CP-MAS spectroscopy

^{27}Al solid-state NMR has been extensively used to probe the local structural characteristics and coordination of aluminum environments in bulk alumina materials.[7] By applying [27]Al magic angle spinning (MAS) experiments, tetra-, penta-, and octahedral aluminum atoms can be revealed.[7, 24] ENREF_7 The signals at 50-80 ppm are usually attributed to tetrahedral aluminums, while those in the range −10 – 20 ppm are assigned to octahedral aluminums.[24] The aluminums in pentahedral coordination exhibit resonances in the 30 – 40 ppm range.[24] Approximately 5% of pentahedral Al-sites can be observed in γ-Al_2O_3 obtained at temperatures above 400 °C.[12, 25] It has been suggested that the pentahedral aluminums are placed mainly on the surface of γ-Al_2O_3.[26]
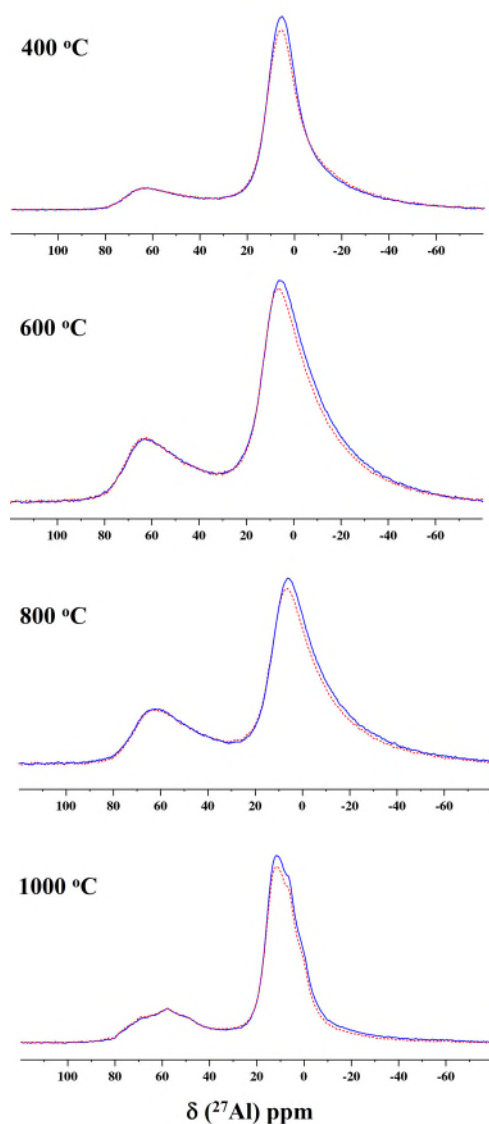
Figure 2. The 9.4 T ^{27}Al MAS NMR spectra of the gibbsite calcined at various temperatures: red-dashed line non-fluorinated sample, blue-solid line fluorinated sample. The broad peak at ca. 10 ppm is assigned to octahedral sites and the less intense peak at around 60 ppm is assigned to tetrahedral sites. Spectra are normalized to have the same peak height of the tetrahedral peaks at ca. 60 ppm.

The 9.4 T ^{27}Al NMR spectra of the gibbsite calcined at various temperatures and then fluorinated are shown in Figure 2. All spectra are obtained under the same experimental conditions so that the spectral features (intensities and widths) can be compared. The spectra reveal well-defined resonances in the region at around 60 and 10 ppm, which are assigned to aluminum in tetrahedral and octahedral coordination, respectively.

The ^{27}Al MAS NMR spectra of the samples obtained at 400 °C show the presence of a broad peak at ca. 10 ppm and the less intense tetrahedral peak at around 60 ppm. In general, boehmite and α-Al$_2$O$_3$ contain aluminum in the octahedral coordination, while in γ-Al$_2$O$_3$, the tetrahedral and octahedral coordination are present at the ratio of ca. 30/70. The ^{27}Al spectrum of the 400 °C specimen reveals the presence of tetrahedral aluminum coordination, although the crystal structure of boehmite contains only one octahedrally coordinated aluminum site. The presence of tetrahedral aluminum could be due to the disordered nature of the boehmite structure caused by fast and violent water expulsion[23] and the presence of γ-Al$_2$O$_3$ in line with the XRD data (Figure 1). The spectral features of the materials calcined up to 600 and 800 °C are very similar and exhibit broader resonances compared to the spectrum of the sample obtained at 400 °C. This is in line with the presence of the γ-Al$_2$O$_3$ phase and the increased structural disorder (Figure 1). The spectra of the gibbsite calcined at 1000 °C (Figure 2) exhibit different and more complex spectral features due to the occurrence of various phases such as α-Al$_2$O$_3$, θ-Al$_2$O$_3$ and δ-Al$_2$O$_3$ (XRD data, Figure 1).

At first sight, the ^{27}Al MAS NMR spectra do not show significant changes due to the HF doping (Figure 2, red dashed line). However, a closer look at the spectra obtained from the HF reacted samples reveals a higher integrated peak intensity ratio of the octahedral to tetrahedral resonances compared to spectra obtained from non-fluorinated material (see Figure 2).[12] This observation suggests a relative increase in the number of octahedral fluorinated aluminum sites and the presence of AlF$_x$O$_{6-x}$ aluminum oxyfluoride species (x = 1, 2). In addition, there is an up-field shoulder, between −10 and −20 ppm, which is more distinctive in the fluorinated samples. The fluorination of Al–O species produces a distortion of the peak at ca 7 ppm as fluorine incorporates into the aluminum oxide matrix, causing line broadening of the up-field part of the resonance.[27] This suggests that, besides the greater presence of octahedral sites, there can be an increase in the disorder in the fluorinated materials resulting in the distributions of bond angles and distances and, consequently, distributions of quadrupolar parameters and the occurrence of a characteristic upfield tail (i.e. towards lower ppm)[7].

The greater ratio of the octahedral to tetrahedral integrated peak intensities in fluorinated samples can suggest a preferential conversion of the coordinatively unsaturated pentahedral[27] and some of tetrahedral[12] reactive sites localized near surface, into octahedral aluminum environments during

fluorination. Calcination produces highly or partly dehydrated surfaces with the presence of trihedral, tetrahedral and pentahedral coordinatively unsaturated sites.[25] These authors reported the significant presence of coordinatively unsaturated tetrahedral and pentahedral sites on the highly dehydrated surface of the alumina calcined at 700 °C.[25] It is postulated that the strongest Lewis-acid sites are trihedral ones, mostly responsible for catalytic activity of γ-Al_2O_3.[28] Knözinger and Ratnasamy predicted the presence of trihedral and pentahedral sites on the surface of dehydrated γ-Al_2O_3[20]. Trihedral aluminum sites have not been detected by NMR in this work, as ^{27}Al MAS NMR has not been very successful in revealing distorted, coordinatively unsaturated three-coordinated aluminum.[29, 30] It was also proposed that highly dehydrated tetrahedral sites could exist on the surface of γ-Al_2O_3.[31, 32] However, the [27]Al signal due to Al^{3+} in tetrahedral surface sites in γ-Al_2O_3 may be very weak or practically undetectable due to the comparatively strong intensity of the bulk tetrahedral [27]Al resonance. On the other hand, the [27]Al signal from Al^{3+} from the surface coordinatively unsaturated pentahedral aluminum is often visible because its presence in bulk is very low. However, ^{27}Al MAS NMR is not capable of distinguishing between the surface and bulk species. Lee *et al*. detected pentahedral aluminum at the surface of hydrated γ-Al_2O_3 at low temperature ($\sim$100 K) and using MAS combined with dynamic nuclear polarization (DNP) to considerably enhance the sensitivity.[33] Note that, due to the field strength, at no stage in the calcining was a signal from pentahedral aluminum detected ^{27}Al MAS NMR (Figure 2). Further work using ultra-high magnetic fields is needed to explore the presence of coordinatively unsaturated species in the γ-Al_2O_3 and their behavior under the fluorination process.

The formation of octahedral fluorinated sites is further explored by an 11.7 T [19]F-[27]Al CP-MAS experiment performed with a short contact time. The short, rotor synchronous contact time of 133 μs used in the [19]F-[27]Al CP-MAS experiments assures that the spectra reveal directly bonded F and Al atoms. For comparison, ^{27}Al MAS NMR (A) and [19]F-[27]Al CP-MAS (B) spectra of the fluorinated gibbsite calcined to 800 °C and ^{27}Al MAS NMR (C) and [19]F-[27]Al CP-MAS (D) spectra of the fluorinated gibbsite calcined to 1000 °C are shown in Figure 3.
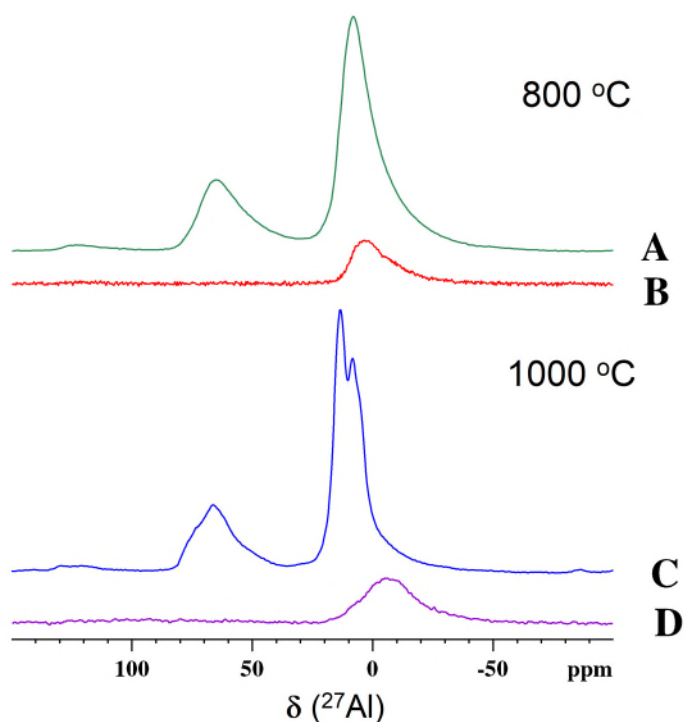
Figure 3. The 11.7 T ^{27}Al NMR spectra of the fluorinated gibbsite calcined to 800 ºC and 1000 ºC: MAS NMR experiments (A) and (C) with 256 transients; ^{19}F-^{27}Al CP-MAS experiments (B) and (D) with 5920 transients. Due to the low signal/noise ratio, the CP-MAS spectra are excessively expanded for the sake of comparison. The ^{19}F radio-frequency field offset frequency was varied to check for the occurrence of ^{27}Al signals from the tetrahedral fluorine structures.

The single resonances that are shown in Figures 3B (ca. 3 ppm) and 3D (ca. −5 ppm) confirm the predominance of the octahedral fluorinated sites. The ^{19}F-^{27}Al CP-MAS spectrum of the fluorinated gibbsite treated at 1000 ºC reveals the peak, which is shifted upfield by 8 ppm (see Figure 3D). This indicates the formation of octahedral aluminum fluoride species, which have different chemical environments compared to the species seen in the fluorinated gibbsite calcined at 800 ºC (see Figure 3B).
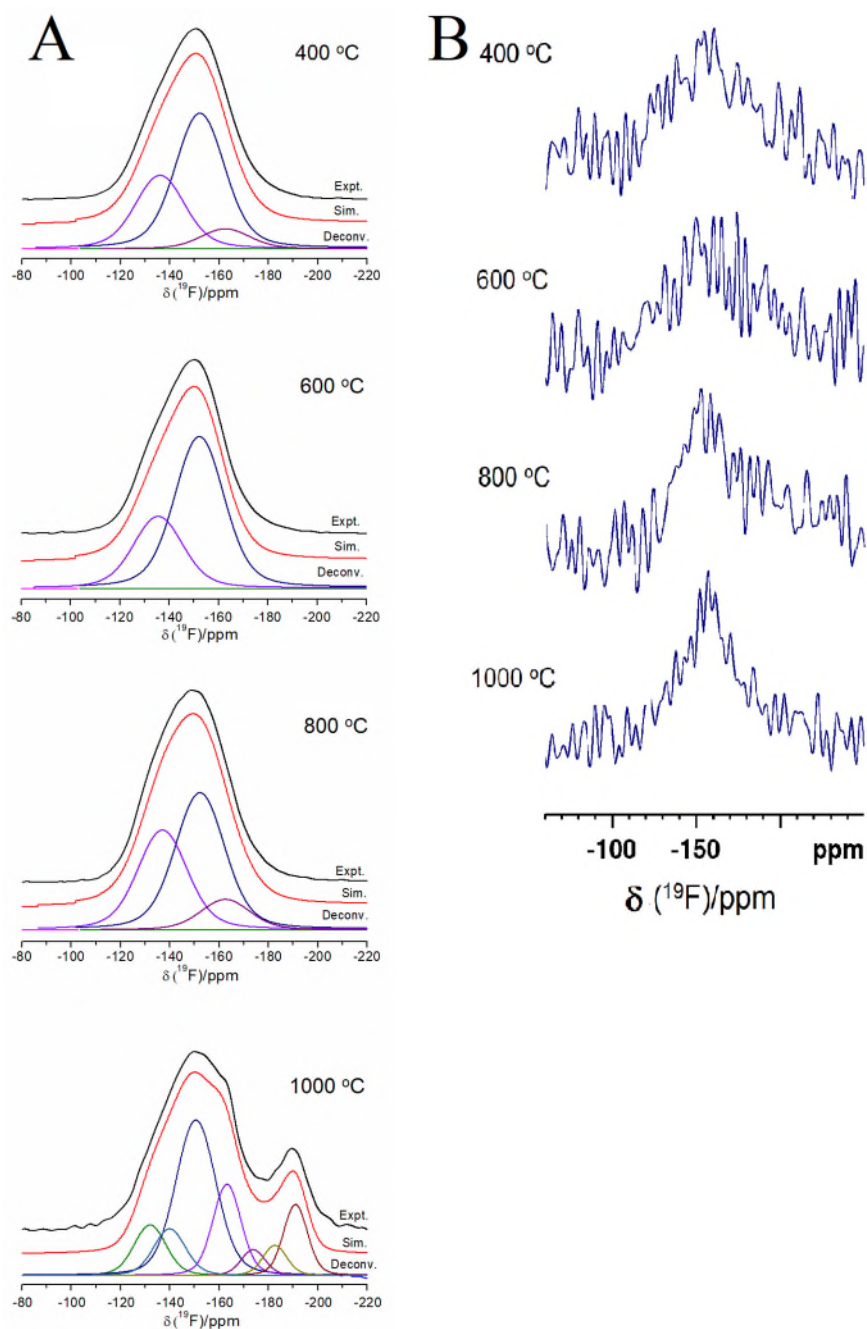
^{19}F MAS NMR spectroscopy

Figure 4. The ^{19}F MAS NMR spectra of the gibbsite calcined at various temperatures indicated in figure: fluorinated (A) and non-fluorinated (B). The spectra can be deconvoluted into Gaussian-Lorentzian lines. Note that several different factors can affect the fluorine chemical shifts, such as fluoride loading, H-F hydrogen bonding, and local geometry.

During the fluorination at lower fluoride loadings, hydroxyl groups on the alumina surface become replaced by fluorine.[11] Knözinger and Ratnasamy[20], Tsyganenko and Mardilovich[4] and Taoufik

et al.[34] proposed various forms of surface hydroxyl groups that can exist on the surface of alumina, depending on the coordination and net electrical charge of the aluminum site. Peri studied dehydrated γ-Al$_2$O$_3$ and F/γ-Al$_2$O$_3$ samples.[35] He reported that dehydration of Al$_2$O$_3$ caused condensation of the Al-OH groups, yielding strained Al-O-Al species (Scheme 1).[35] At low fluoride loadings the fluoride preferentially interacts with the Lewis acid center of the strained Al-O-Al species as presented in Scheme 1.[35] Higher fluoride loadings cause bridging Al-O-Al bonds to break and adsorb more fluorine, forming the Al-F-Al bonds.[11]
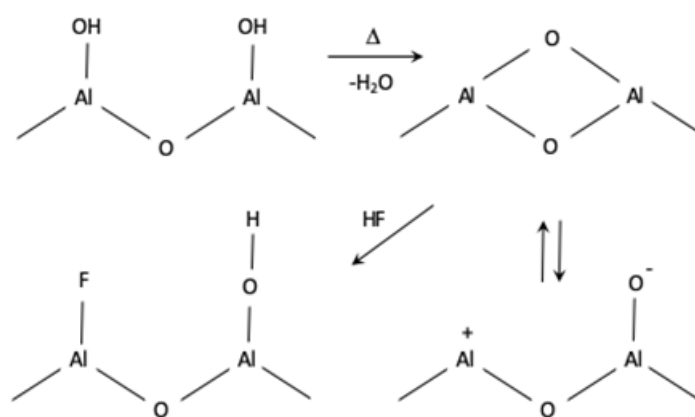
Scheme 1. Dehydration of Al$_2$O$_3$ and the reaction of HF with Al$_2$O$_3$, adapted from ref.[36]

Padhye *et al.* used Density Functional Theory (DFT) calculations to study exothermic surface chemistry between alumina and fluorinated species which replaced a surface hydroxyl group attached to an aluminum atom.[37] These authors assumed surface hydroxyl sites similar to those presented by Knözinger and Ratnasamy.[20] DFT calculations indicated that terminal OH groups possessed greater reactivity. DeCanio *et al.* used ^{1}H NMR to study the hydroxyl structure of γ-Al$_2$O$_3$ and fluoride altered γ-Al$_2$O$_3$ materials.[38] In their work, SSNMR of γ-Al$_2$O$_3$ calcined at 700 °C exhibited five different types of hydroxyl groups in line with the work of Knözinger and Ratnasamy.[20] The hydroxyl groups have slightly different net charges which determine their Brønsted acidity. Upon fluorination, the most basic hydroxyl groups (directly attached to the six- and four coordinated aluminums) with the highest net negative charge are preferentially replaced by fluorine.

The ^{19}F MAS NMR spectra of gibbsite calcined at various temperatures (400, 600, 800 and 1000 °C) and then reacted with HF are shown in 4B and 4A, respectively. The chemical shift positions

of the deconvoluted peaks, together with their integrated peak intensities are summarized in Table 1. The ^{19}F MAS NMR spectra of gibbsite calcined up to 800 °C shown in Figure 4, exhibit very similar, broad and slightly asymmetric peaks which can be well deconvoluted into three resonances (400 and 800 °C) centered at ca. −137, −153 and −164 ppm and two resonances (600 °C) centered at ca. −136 and −151 ppm. The shape of the broad peaks implies the complex nature of the materials and the superposition of different structures of fluorine species bound to one, two, and three octahedral aluminum atoms.[11] Zhang *et al*. assigned the high field peak (−161 ppm) to the terminal Al-F octahedral surface sites (S1, see Scheme 2), while the low field peaks (−145, −132 ppm) were assigned to bridging Al-F octahedral surface sites (S2, S3, respectively see Scheme 2). ENREF 8[11] The concept of the assignment presented in Zhang *et al*.[11, 39] was based on the model of Knözinger and Ratnasamy[20] which envisages the presence of various OH groups in surface layers of aluminas.

Considering the low level of fluorination presented in this work (i.e. 1.3 – 2.3 wt %F), it is expected that fluorine is firstly replacing the surface hydroxyl groups (terminal position) without breaking Al-O-Al bonds and without entering into the alumina framework, creating mostly S1 species (peak at ca. −160 ppm). By further diffusion into the alumina framework fluoride produces bridging Al-O-Al bonds species (S2 at ca. 150 and S3 at ca. 135 ppm).[11] According to the assignment by Zhang *et al*.[11] the most prominent species detected in this work would be the S2 species. However, due to the complex nature of fluorine adsorption and the low fluorine loadings, it is only possible to present tentative peak assignments and the intensity ratios.

Table 1. Chemical shifts and relative fractions of fluorinated species identified by the deconvolution of ^{19}F MAS NMR spectra. Linewidths of the simulated peaks in the spectra of fluorinated gibbsites calcined at 400 – 800 °C are 25-30 ppm, while for the sample calcined at 1000 °C, linewidths are 8-18 ppm.

Calcine temperature	Component peak number and ^{19}F chemical shift δ (ppm) ±0.5 ppm / Integrated peak intensity (fractions) ±0.01												
Sample	1		2		3		4		5		6		7	
400 °C	−137.0	0.30	−153.2	0.60	−164.8	0.10								
600 °C	−136.5	0.30	−151.5	0.70										
800 °C	−138.0	0.40	−153.2	0.50	−163.5	0.10								
1000 °C	−132.0	0.10	−139.9	0.10	−150.6	0.40	−163.2	0.2	−173.0	0.05	−182.6	0.05	−191.0	0.10
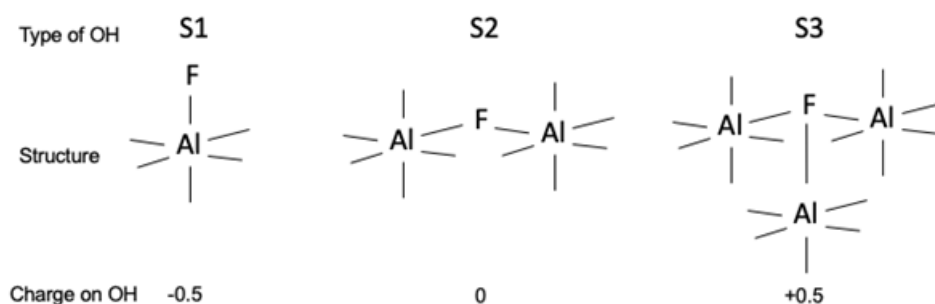
Scheme 2. Possible structures of fluorine species located on the surfaces of fluorinated gibbsite ENREF_9 specimens calcined at different temperatures. Charge on precursor OH groups from ref.[11]

The ratio of the present integrated peak intensities is similar for the entire calcine temperature sequence up to 800 °C (Table 1). This means that the available structures at the surface for fluorination of gibbsite calcined in the 400 °C – 800 °C range are comparable. As expected, the ^{19}F MAS NMR spectrum of the fluorinated gibbsite treated at 1000 °C is more complex, and the deconvolution reveals seven peaks (Table 1), including two peaks, which can be seen in the previous spectra at ca. −132 and −150 ppm. Apart from these, there are additional resonances at ca. −139, −164, −176, −183 and −191 ppm. The more complex ^{19}F MAS NMR spectrum of the fluorinated gibbsite treated at 1000 °C is the result of the presence of different phases such as δ-, θ- and α- aluminas (see Figure 1). The resonances in the chemical shift range −130 – −165 ppm are in line with the presence of various fluorine species bound to octahedral aluminum atoms (see Figure 3D and Scheme 2). Chupas *et al*. assigned the

resonance at −172 ppm to bulk anhydrous aluminum fluoride obtained at the very high fluorine loadings.[40] However, in this work due to relatively low fluorine loading, the peak at −175.9 ppm is more likely to originate from terminal fluorine groups. The peaks in the chemical shift range of about −180 − − 200 ppm can be either also attributed to terminal fluorine species[12] or to cryolite (Na_3AlF_6) and/or chiolite ($Na_5Al_3F_{14}$).[17] The presence of multiple new features is consistent with XRD findings, demonstrating a conversion from predominantly γ-Al_2O_3 to a material rich in δ-, θ- and α-Al_2O_3 phases at 1000 °C (Figure 1). It is also possible that the upfield peaks can be associated with fluorinated sodium impurities dispersed throughout the crystal lattice that are strongly surface segregated in the gibbsite calcined at 1000 °C.[41, 42] The XPS analysis provides evidence of Na-F interactions in similar materials which were analogously treated.[43] Dando has demonstrated that sodium fluoroaluminate compounds cryolite and chiolite show a resonance centered at −189 ppm in ^{19}F MAS NMR spectra.[17]

Conclusions

A series of gibbsite specimens calcined at temperatures 400 − 1000 °C were analyzed before and after contact with anhydrous HF. Gibbsite specimens obtained at 600 and 800 °C were dominated by γ-Al_2O_3, while those produced at 1000 °C showed the presence of α-Al_2O_3, and other phases such as θ-Al_2O_3 and δ-Al_2O_3, which is confirmed by XRD. ^{19}F MAS NMR and ^{27}Al MAS NMR and ^{19}F-^{27}Al CP-MAS spectra reveal the formation of new octahedral species after fluorination. These structures have been formed partly due to the consumption of tetrahedral sites and the replacement of OH groups in octahedral species. The presence of a range of different oxyfluoride sites in the gibbsite calcined at 1000 °C samples is indicative of very different surface chemistry on θ-, δ- and α-Al_2O_3. Three types of Al-F species on the surface of fluorinated gibbsite specimens calcined at 400, 600, 800 °C are presented based on the ^{19}F NMR spectra and the peaks detected at ca. −135, −151 and −163 ppm. Their formation is explained partly by breaking Al-O-Al bonds and the elementary exchange reactions in which -OH groups with different basicity are replaced by F^-. The presence of the same groups and the corresponding relative integrated peak intensities suggests a similar process of fluorination in all

gibbsite specimens calcined up to 800 °C. In the ^{19}F MAS NMR spectrum of the fluorinated gibbsite calcined at 1000 ^{o}C in addition to peaks at ca. −133 and −151 ppm, five additional peaks are detected at ca. −139, −164, −176, −183 and −191 ppm. They are assigned to fluorine species bound to one, two, and three octahedral aluminum atoms (−133 – −164 ppm) terminal fluorine groups (−176 ppm), terminal fluorine species or, the cryolite and chiolite (−183 and −191 ppm).

Declaration of Competing Interest

The authors declare that they have no known competing financial interests or personal relationships that could have appeared to influence the work reported in this paper.

References

(1) Donaldson, D.; Raahauge, B., *Essential Readings in Light- Metals*. Springer International Publishing AG: Switzerland, 2016; Vol. Volume 1: Alumina and Bauxite, p 1169.

(2) Trueba, M.; Trasatti, S. P. γ-Alumina as a Support for Catalysts: A Review of Fundamental Aspects. *Eur. J. Inorg. Chem.* **2005,** *2005* (17), 3393-3403.

(3) Busca, G. Silica-alumina catalytic materials: A critical review. *Catal. Today* **2019**.

(4) Tsyganenko, A. A.; Mardilovich, P. P. Structure of alumina surfaces. *J. Chem. Soc., Faraday Trans.* **1996,** *92* (23), 4843-4852.

(5) Grjotheim, K.; Welch, B. J., *Aluminium smelter technology : a pure and applied approach*. Aluminium-Verlag: Düsseldorf, 1988.

(6) *Light metals: proceedings of the technical sessions presented by the TMS Aluminum Committee at the 135th TMS annual meeting, San Antonio, Texas, USA, March 12 - 16, 2006*. TMS (The Minerals, Metals & Materials Society);: Warrendale, Pa., 2006.

(7) Mackenzie, K.; Smith, M., *Multinuclear Soild-State NMR of Inorganic Materials*. Pergamon: 1st edition, Oxford OX5 1GB, UK, 2002.

(8) Fischer, L.; Harlé, V.; Kasztelan, S.; d'Espinose de la Caillerie, J. B. Identification of fluorine sites at the surface of fluorinated γ-alumina by two-dimensional MAS NMR. *Solid State Nucl. Magn. Reson.* **2000,** *16* (1), 85-91.

(9) König, R.; Scholz, G.; Bertram, R.; Kemnitz, E. Crystalline aluminium hydroxy fluorides—Suitable reference compounds for 19F chemical shift trend analysis of related amorphous solids. *J. Fluorine Chem.* **2008,** *129* (7), 598-606.

(10) König, R.; Scholz, G.; Pawlik, A.; Jäger, C.; van Rossum, B.; Oschkinat, H.; Kemnitz, E. Crystalline Aluminum Hydroxy Fluorides: Structural Insights Obtained by High Field Solid State NMR and Trend Analyses. *J. Phys. Chem. C* **2008,** *112* (40), 15708-15720.

(11) Zhang, W.; Sun, M.; Prins, R. Multinuclear MAS NMR Identification of Fluorine Species on the Surface of Fluorinated γ-Alumina. *J. Phys. Chem. B* **2002,** *106* (45), 11805-11809.

(12) Chupas, P. J.; Grey, C. P. Surface modification of fluorinated aluminas: Application of solid state NMR spectroscopy to the study of acidity and surface structure. *J. Catal.* **2004,** *224* (1), 69-79.

(13) Scalise, V.; Scholz, G.; Bertram, R.; Kemnitz, E. Identification of F- species after adsorption at the surface of milled and unmilled γ-Al2O3. *Surf. Interfaces* **2018,** *10*, 117-122.

(14) König, R.; Scholz, G.; Pawlik, A.; Jäger, C.; van Rossum, B.; Kemnitz, E. Identification of AlFx(OR)y Species in Strongly Disordered Aluminum Isopropoxide Fluoride Solids: A Field-Dependent MAS NMR Study. *J. Phys. Chem. C* **2009,** *113* (35), 15576-15585.

(15) Ahrem, L.; Scholz, G.; Bertram, R.; Kemnitz, E. Thermal Evolution of 4- and 5-fold Coordinated Al-Sites in Aluminum Hydroxide Fluorides with Low Fluorination Degree. *J. Phys. Chem. C* **2016,** *120* (17), 9236-9244.

(16) Chupas, P. J.; Ciraolo, M. F.; Hanson, J. C.; Grey, C. P. In Situ X-ray Diffraction and Solid-State NMR Study of the Fluorination of γ-Al2O3 with HCF2Cl. *J. Am. Chem. Soc.* **2001,** *123* (8), 1694-1702.

(17) Dando, N. R. Adsorption/Entrainment of fluroride in smelting grade alumina: surface chemical speciation and adsorption mechanism. *Light Metals TMS* **2005**, 133.

(18) Yang, Y. J.; Hyland, M.; Wang, Z. W.; Seal, C. Modelling HF generation in aluminium reduction cell. *Can. Metall. Q.* **2015,** *54* (2), 149-160.

(19) Wefers, K.; Misra, C. Oxides and Hydroxides of Aluminum. *Alcoa Technical Paper* **1987,** *19*, 92.

(20) Knözinger, H.; Ratnasamy, P. Catalytic Aluminas: Surface Models and Characterization of Surface Sites. *Catal. Rev.* **1978,** *17* (1), 31-70.

(21) Perander, L. M.; Stam, M. A.; M., H. M.; JMetson, J. B., Towards Redefining the Alumina Specifications Sheet - the Case of HF Emissions. In *Light Metals,* Edited by: Stephen J. Lindsay TMS (The Minerals, Metals & Materials Society), 2011

(22) Vega, A. J. CPMAS of quadrupolar S = 32 nuclei. *Solid State Nucl. Magn. Reson.* **1992,** *1* (1), 17-32.

(23) Hill, M. R.; Bastow, T. J.; Celotto, S.; Hill, A. J. Integrated Study of the Calcination Cycle from Gibbsite to Corundum. *Chem. Mater.* **2007,** *19* (11), 2877-2883.

(24) Perander, L. M.; Zujovic, Z. D.; Groutso, T.; Hyland, M. M.; Smith, M. E.; O Dell, L. A.; Metson, J. B. Characterization of metallurgical-grade aluminas and their precursors by 27Al NMR and XRD. *Can. J. Chem.* **2007,** *85* (10), 889-897.

(25) Ahrem, L.; Scholz, G.; Gutmann, T.; Calvo, B.; Buntkowsky, G.; Kemnitz, E. Direct Observation of Coordinatively Unsaturated Sites on the Surface of a Fluoride-Doped Alumina Catalyst. *J. Phys. Chem. C* **2017,** *121* (22), 12206-12213.

(26) Kwak, J. H.; Hu, J. Z.; Kim, D. H.; Szanyi, J.; Peden, C. H. F. Penta-coordinated Al3+ ions as preferential nucleation sites for BaO on γ-Al2O3: An ultra-high-magnetic field 27Al MAS NMR study. *J. Catal.* **2007,** *251* (1), 189-194.

(27) Marshall, C. P.; Scholz, G.; Braun, T.; Kemnitz, E. Strong Lewis acidic catalysts for C–F bond activation by fluorination of activated γ-Al2O3. *Catal. Sci. Technol.* **2020,** *10* (2), 391-402.

(28) Wischert, R.; Copéret, C.; Delbecq, F.; Sautet, P. Optimal Water Coverage on Alumina: A Key to Generate Lewis Acid–Base Pairs that are Reactive Towards the C☐H Bond Activation of Methane. *Angew. Chem. Int. Ed.* **2011,** *50* (14), 3202-3205.

(29) Sanchez Escribano, V.; Garbarino, G.; Finocchio, E.; Busca, G. γ-Alumina and Amorphous Silica–Alumina: Structural Features, Acid Sites and the Role of Adsorbed Water. *Top. Catal.* **2017,** *60* (19), 1554-1564.

(30) Chen, F. R.; Davis, J. G.; Fripiat, J. J. Aluminum coordination and Lewis acidity in transition aluminas. *J. Catal.* **1992,** *133* (2), 263-278.

(31) Digne, M.; Sautet, P.; Raybaud, P.; Euzen, P.; Toulhoat, H. Use of DFT to achieve a rational understanding of acid–basic properties of γ-alumina surfaces. *J. Catal.* **2004,** *226* (1), 54-68.

(32) Busca, G. Spectroscopic characterization of the acid properties of metal oxide catalysts. *Catal. Today* **1998,** *41* (1), 191-206.

(33) Lee, D.; Duong, N. T.; Lafon, O.; De Paëpe, G. Primostrato Solid-State NMR Enhanced by Dynamic Nuclear Polarization: Pentacoordinated Al3+ Ions Are Only Located at the Surface of Hydrated γ-Alumina. *J. Phys. Chem. C* **2014,** *118* (43), 25065-25076.

(34) Taoufik, M.; Szeto, K. C.; Merle, N.; Rosal, I. D.; Maron, L.; Trébosc, J.; Tricot, G.; Gauvin, R. M.; Delevoye, L. Heteronuclear NMR Spectroscopy as a Surface-Selective Technique: A Unique Look at the Hydroxyl Groups of γ-Alumina. *Chem. Eur. J.* **2014,** *20* (14), 4038-4046.

(35) Peri, J. B. Effect of fluoride on surface "acid" sites on .gamma.-alumina and silica-alumina. *J. Phys. Chem.* **1968,** *72* (8), 2917-2925.

(36) Decanio, E.; Bruno, J. W.; Nero, V. P.; Edwards, J. C. 27Al NMR, FT-IR and Ethanol-18O TPD Characterization of Fluorided Alumina. *J. Catal.* **1993,** *140* (1), 84-102.

(37) Padhye, R.; Aquino, A. J. A.; Tunega, D.; Pantoya, M. L. Fluorination of an Alumina Surface: Modeling Aluminum–Fluorine Reaction Mechanisms. *ACS Appl. Mater. Interfaces* **2017,** *9* (28), 24290-24297.

(38) Decanio, E. C.; Edwards, J. C.; Bruno, J. W. Solid-State 1H MAS NMR Characterization of γ-Alumina and Modified γ-Aluminas. *J. Catal.* **1994,** *148* (1), 76-83.

(39) Zhang, W.; Sun, M.; Prins, R. A High-Resolution MAS NMR Study of the Structure of Fluorinated NiW/γ-Al2O3 Hydrotreating Catalysts. *J. Phys. Chem. B* **2003,** *107* (40), 10977-10982.

(40) Chupas, P. J.; Corbin, D. R.; Rao, V. N. M.; Hanson, J. C.; Grey, C. P. A Combined Solid-State NMR and Diffraction Study of the Structures and Acidity of Fluorinated Aluminas: Implications for Catalysis. *J. Phys. Chem. B* **2003,** *107* (33), 8327-8336.

(41) McIntosh, G. J.; Wijayaratne, H.; Chan, A.; Perander, L.; Hyland, M. On the mechanism of sodium migration in transition aluminas with calcination. *Acta Mater.* **2018,** *153*, 226-234.

(42) McIntosh, G. J.; Chan, A. Probing hydrogen bonding interactions and impurity intercalation in gibbsite using experimental and theoretical XANES spectroscopy. *Phys. Chem. Chem. Phys.* **2018,** *20* (37), 24033-24044.

(43) Haverkamp, R. G.; Metson, J. B.; Hyland, M. M.; Welch, B. J. Adsorption of hydrogen fluoride on alumina. *Surf. Interface Anal.* **1992,** *19* (1-12), 139-144.